

# The Stable Isotope Hydrology of Sable Island, NS, Canada

Geoff Koehler<sup>1</sup> and Keith Hobson<sup>2</sup>

<sup>1</sup>NHRC Stable Isotope Laboratory

<sup>2</sup>Environment Canada

November 22, 2022

## Abstract

We investigated the stable isotope hydrology of Sable Island, NS, Canada over a four year period from September, 2017 until August, 2021. The  $\delta$  2 H and  $\delta$  18 O values of integrated monthly precipitation were weakly seasonal and ranged from -66 to -17 per mil and from -9.7 to -3.1 per mil, respectively. Fitting these monthly precipitation data resulted in a Local Meteoric Water Line (LMWL) defined by:  $\delta$  2 H =  $7.28 \pm 0.22 \times \delta$  18 O +  $7.95 \pm 1.38$  per mil. Amount weighted annual precipitation had  $\delta$  2 H and  $\delta$  18 O values of  $-37 \pm 12$  per mil and  $-6.1 \pm 1.6$  per mil, respectively. Deep groundwater had more negative  $\delta$  2 H and  $\delta$  18 O values than mean annual precipitation, suggesting recharge occurs mainly in the winter, while shallow groundwater had  $\delta$  2 H and  $\delta$  18 O values more consistent with mean annual precipitation or mixing of freshwater with local seawater. Surface waters had more positive values and showed evidence of isolation from the groundwater system. The stable isotopic compositions of plant(leaf) water, on the other hand, indicate plants use groundwater as their source. Fog had  $\delta$  2 H and  $\delta$  18 O values that were significantly more positive than those of local precipitation, yet had similar 17 O-excess values. Our results establish an important framework for ongoing isotopic studies of feral horses and other wildlife on Sable Island.



## Abstract

We investigated the stable isotope hydrology of Sable Island, NS, Canada over a four year period from September, 2017 until August, 2021. The  $\delta^2\text{H}$  and  $\delta^{18}\text{O}$  values of integrated monthly precipitation were weakly seasonal and ranged from -66 to -17 per mil and from -9.7 to -3.1 per mil, respectively. Fitting these monthly precipitation data resulted in a Local Meteoric Water Line (LMWL) defined by:  $\delta^2\text{H} = 7.28 \pm 0.22 \times \delta^{18}\text{O} + 7.95 \pm 1.38$  per mil. Amount weighted annual precipitation had  $\delta^2\text{H}$  and  $\delta^{18}\text{O}$  values of  $-37 \pm 12$  per mil and  $-6.1 \pm 1.6$  per mil, respectively. Deep groundwater had more negative  $\delta^2\text{H}$  and  $\delta^{18}\text{O}$  values than mean annual precipitation, suggesting recharge occurs mainly in the winter, while shallow groundwater had  $\delta^2\text{H}$  and  $\delta^{18}\text{O}$  values more consistent with mean annual precipitation or mixing of freshwater with local seawater. Surface waters had more positive values and showed evidence of isolation from the groundwater system. The stable isotopic compositions of plant(leaf) water, on the other hand, indicate plants use groundwater as their source. Fog had  $\delta^2\text{H}$  and  $\delta^{18}\text{O}$  values that were significantly more positive than those of local precipitation, yet had similar  $^{17}\text{O}$ -excess values. Our results establish an important framework for ongoing isotopic studies of feral horses and other wildlife on Sable Island.

## 1 Introduction

Measurements of the stable isotopic compositions of hydrogen and oxygen in environmental waters have long been recognized as an important tool for tracing water origins and evaluating the hydrology of regions at local and continental scales (Craig, 1961; Dansgaard, 1964; Clark & Fritz, 1997). This approach is based on the fundamental principles of isotopic tracing involving knowledge of source water isotopic endmembers and the isotopic composition of waters associated with mixing and/or measured or predicted isotopic effects of evapotranspiration (Gonfiantini, 1986). The establishment of a Local Meteoric Water Line (LMWL), or the absolute relationship between  $\delta^2\text{H}$  and  $\delta^{18}\text{O}$  in precipitation at study sites will typically differ from the Global Meteoric Water line (GMWL) of Craig (1961), due to varying regional climatic and geographic parameters. These differences are a consequence of differential fractionation of hydrogen and oxygen isotopes in response to relative humidity during primary evaporation along with temperature and secondary evaporation effects (Craig & Gordon, 1965; Gonfiantini et al., 2018). Because of these processes, the measured  $\delta^2\text{H}$  and  $\delta^{18}\text{O}$  values of precipitation at different locations will produce different meteoric water lines. Relationships between  $\delta^2\text{H}$  and  $\delta^{18}\text{O}$  in surface and groundwater as well as plant leaf water can differ from the LMWL but the intercept of such relationships and the LMWL can reveal the ultimate source of water driving these pools.

Applications related to isotope hydrology are vast and have clearly informed a number of studies on abiotic and biotic processes. Among biological investigations, the field of hydroecology has been a fundamental addition to studies formally evaluating sources of water to foodwebs (Baxter et al., 2005; Meier-Augenstein, 2011). The use of isotopic measurements of water to establish key ecological information such as plant water uptake (Edwin et al., 2014) and water sources used by animals (Wolf et al., 2002; Vander Zanden et al., 2016) are now well established. More recently, measurements of  $\delta^{17}\text{O}$  in environmental waters have been used together with  $\delta^{18}\text{O}$  to provide additional information on sources of water and mechanisms of transport related to differential involvement of kinetic *vs.* equilibrium fractionation (Tian et al., 2021). As an example of this, fog and dew may be differentiated from precipitation using the relationship between their  $\delta^{17}\text{O}$  and  $\delta^{18}\text{O}$  values (Kaseke et al., 2017).

In this paper, we examine baseline isotopic information of precipitation, fog, surface waters, plantwater, and groundwater on Sable Island, a narrow sandbar in the open north Atlantic Ocean approximately 150 km east of Nova Scotia, Canada. Our

68 motivation was to provide a framework to examine the integrity of the freshwater supply  
69 on the island and, ultimately, to assist us in understanding water use by vegetation  
70 and the iconic wild horses that persist on Sable Island (Plante et al., 2007; Freedman  
71 et al., 2011; McLoughlin et al., 2016). From a stable isotope ecology perspective, this  
72 isolated environment offers an ideal opportunity to study the routing of the stable isotopes  
73 of hydrogen and oxygen from water to animal tissues. Here, we present the first  
74 component of this work and focus on isotopically describing different water sources  
75 that form the primary reservoir of water that may be integrated by horses specifically,  
76 but also by other flora and fauna on the island.

## 77 2 Methods

### 78 2.1 Study Site

79 Sable Island is the only unsubmerged part of the Sable Island Bank, a series of  
80 sandbanks and shoals that border the Atlantic continental shelf and extend from Baffin  
81 Bay to the Gulf of Maine (Fig. 1). Historically, Sable Island was a notorious shipping  
82 hazard. The island is often subject to extreme weather for a large part of the year  
83 including high winds, breaking seas, and thick fog. This, coupled with strong ocean  
84 currents and its close proximity to shipping lanes, has resulted in the accumulation  
85 of hundreds of shipwrecks, the last of which was in 1999 (Stalter & Lamont, 2006).  
86 In modern times, however, it is most widely known for its population of feral horses  
87 (*Equus ferus caballus*), whose ancestors were introduced to the island in the mid 18th  
88 century (Freedman et al., 2011). Because of their long tenure on the island, these Sable  
89 Island Horses are considered genetically distinct (Plante et al., 2007) and the entire  
90 Sable Island ecosystem, including its horses, is protected as Sable Island National  
91 Park Reserve by Parks Canada. Because of this unique and isolated environment,  
92 Sable Island has been the focus of many scientific studies. These have mainly focused  
93 on the peculiar ecology of the feral horse population, but other investigations have  
94 ranged from traditional hydrology (Hennigar & Kennedy, 2016; Hennigar, 1976) to  
95 plant ecology (Tissier et al., 2013; Richardson et al., 2009).

96 Sable Island’s climate is classified in the updated Köppen-Geiger climate classification  
97 as Dfb (cold with a warm summer, but lacking a dry season) (Eamer et al.,  
98 2021). Temperatures range from about 0 °C in the winter to highs of about 25 °C in  
99 the summer months (Stalter & Lamont, 2006). Sable Island receives approximately  
100 1460 mm of precipitation, mainly rain, annually (Environment and Climate Change  
101 Canada, 2021). This relatively large amount of rainfall along with high infiltration  
102 and no run-off results in an island-wide discontinuous unconfined freshwater aquifer,  
103 essentially a fresh water lens, diffusing into the sea at the lateral margins of the island  
104 (Hennigar & Kennedy, 2016). Vegetation consists mostly of marram grass (*Ammophila  
105 arenaria*) however as many as 224 species of vascular plants have been identified, both  
106 native and introduced (Stalter & Lamont, 2006).

### 107 2.2 Water and Plant Collections

108 As part of an ongoing project, we collected monthly integrated precipitation  
109 using a Palmex integrator (Gröning et al., 2012) at the Parks Canada Station on  
110 Sable Island operated by the Meteorological Survey of Canada for four years, from  
111 September 2017 to August 2021. In addition to the precipitation samples, we collected  
112 monthly groundwater samples from the deep freshwater well (screened at 5 meters)  
113 that supplies the main station on the western spit of the island (Fig 1-inset) during  
114 the same time period. We also collected opportunistic pond, lake, and shallow well  
115 water samples from various locations on the island. Fog samples were collected using  
116 a fog collector constructed after Fischer and Still (2007), but using the same model of  
117 Palmex integrator for the sample collection reservoir. Precipitation amounts and other

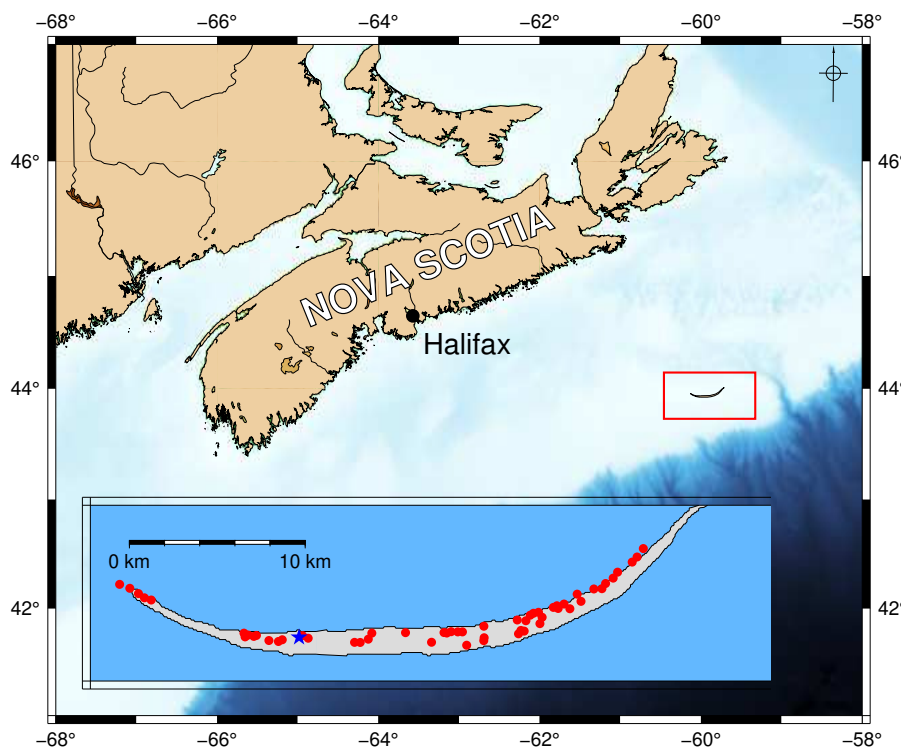


**Figure 1.** Location of Sable Island, NS, Canada, showing the locations of marram grass samples (red circles). The blue star indicates the location of the main Parks Canada Station where precipitation samples and deep groundwater were collected.

118 meteorological data were obtained from Environment and Climate Change Canada  
 119 (Environment and Climate Change Canada, 2021).

120 In addition to the water samples, we collected samples of marram grass into dou-  
 121 ble ziplock plastic bags (Fig 1-inset). Plant water was cryogenically extracted following  
 122 the procedures of Koeniger et al. (2011) at the Global Institute for Water Security Lab-  
 123 oratory at the University of Saskatchewan. This system was composed of independent  
 124 extraction-collection units made up of two Exetainer vials (Labco Ltd, Lampeter, UK)  
 125 connected by a stainless steel capillary ( $2.00 \times 0.95$  mm). The samples were heated to  
 126  $200\text{ }^{\circ}\text{C}$  for 15 min under a baseline vacuum pressure of 87.0 Pa. The volatile fraction  
 127 in the plant sample was vaporized and collected in the second Exetainer vial, set in a  
 128 liquid nitrogen cold trap. The samples were defrosted at room temperature in sealed  
 129 conditions and the collected liquid was sampled for isotopic analysis. Extraction effi-  
 130 ciency was determined gravimetrically and samples with an extraction efficiency of  
 131 less than is 96% were rejected.

### 132 2.3 Stable Isotope Measurements

133 All precipitation, groundwater, and plant water samples were measured for their  
 134 hydrogen and oxygen stable isotopic compositions at the NHRC Stable Isotope Lab-  
 135 oratory in Saskatoon, SK, and are reported in the familiar delta notation on the  
 136 VSMOW–SLAP reference scale. Precipitation and groundwater samples were mea-  
 137 sured by Off Axis Integrated Cavity Output Spectroscopy (OA-ICOS) using either a  
 138 Los Gatos Research EP-45 triple isotope laser spectrometer or a Los Gatos Research  
 139 DLT-100 dual isotope laser spectrometer. To minimize memory effects, samples and

140 reference waters were injected 9 times and the last 5 measurements were averaged to  
 141 obtain the final raw delta values.

142 To avoid spectral interferences caused by co-extracted organic compounds (Millar  
 143 et al., 2021), plant water samples were measured by Isotope Ratio Mass Spectroscopy  
 144 (IRMS) with an Elementar Isoprime mass spectrometer. For oxygen isotope analyses,  
 145 we used the CO<sub>2</sub>-H<sub>2</sub>O equilibration technique of Epstein and Mayeda (1953) with an  
 146 Elementar multi-flow peripheral device. Samples were allowed to equilibrate with CO<sub>2</sub>  
 147 for at least 48 hours prior to measurement. For hydrogen isotope analyses, we reacted  
 148 water with elemental Cr at 1030 °C followed by IRMS measurement of the produced  
 149 H<sub>2</sub> (Morrison et al., 2001). To alleviate memory effects, samples were injected twice  
 150 and the first measurement discarded.

151 For both laser and IRMS analyses, we used two calibrated reference waters,  
 152 (CSNOW  $\delta^2\text{H} = -204.7$ ,  $\delta^{18}\text{O} = -26.9$  and LVIC (Lake Victoria)  $\delta^2\text{H} = +10.0$ ,  $\delta^{18}\text{O} =$   
 153  $+0.47$  per mil, respectively) to normalize raw delta values to the VSMOW–SLAP scale.  
 154 Precisions as determined by replicate analyses of samples and reference waters were  $\pm$   
 155  $1$  for  $\delta^2\text{H}$  and  $\pm 0.1$  per mil for both  $\delta^{17}\text{O}$  and  $\delta^{18}\text{O}$  values. For  $\delta^{17}\text{O}$  measurements, we  
 156 calibrated our CSNOW and LVIC reference waters on the SMOW-SLAP scale following  
 157 the procedures proposed by Schoenemann et al. (2013), whereby the VSMOW2 and V-  
 158 SLAP2 reference waters supplied by the IAEA are assumed to have <sup>17</sup>O-excess values  
 159 of 0. Following this procedure, our LVIC and CSNOW reference waters have  $\delta^{17}\text{O}$   
 160 values of  $+0.1$  and  $-14.1$  per mil, respectively.

## 161 2.4 Statistical Analysis

162 We used the R programming language for all statistical calculations (R Core  
 163 Team, 2015). The amount-weighted mean  $\delta^2\text{H}$  and  $\delta^{18}\text{O}$  values of precipitation can  
 164 be calculated following Yurtsever and Gat (1981):

$$\delta_w = \frac{\sum_{i=1}^n P_i \delta_i}{\sum_{i=1}^n P_i} \quad (1)$$

165 where for each measurement, P is the precipitation amount and  $\delta$  is its  $\delta^2\text{H}$  or  $\delta^{18}\text{O}$   
 166 value. Deuterium excess ( $D_{ex}$ ) values were calculated following Dansgaard (1964):

$$D_{ex} = \delta^2\text{H} - 8\delta^{18}\text{O} \quad (2)$$

167 Local meteoric water lines are most often calculated using ordinary least squares  
 168 regression (OSLR) to model the relationship between  $\delta^{18}\text{O}$  and  $\delta^2\text{H}$  values assuming  
 169 that each point carries equal weight (IAEA, 1992). Amount weighted models (either  
 170 OLSR or Major Axis regressions) can also be used to model the LMWL (Hughes &  
 171 Crawford, 2012; Crawford et al., 2014). While useful in certain circumstances, these  
 172 alternate approaches are most applicable to locations where there are an abundance  
 173 of small evaporative precipitation events that would otherwise skew the LMWL to  
 174 shallower slopes and a less positive deuterium intercept.

## 175 3 Results and Discussion

### 176 3.1 Meteoric waters

177 The hydrogen and oxygen stable isotopic compositions of precipitation on Sable  
 178 Island have  $\delta^2\text{H}$  values that ranged from  $-66$  to  $-15$  per mil and  $\delta^{18}\text{O}$  values that  
 179 range from  $-9.7$  to  $-1.9$  per mil. Correlations between the hydrogen stable isotopic

model	slope	Intercept(‰)	r <sup>2</sup>
OLSR	7.28 ± 0.22	7.95 ± 1.38	0.956
PW-OLSR	7.37 ± 0.26	8.44 ± 1.63	0.947
RMA	7.60 ± 0.33	9.84 ± 1.96	0.956

**Table 1.** Modelling of the local meteoric water line for Sable Island, NS. OLSR - Ordinary Standard Linear regression, PW-OSLR - Precipitation Weighted – Ordinary Standard Linear Regression, RMA - Reduced Mean Axis regression.

180 compositions and amount of precipitation (Fig. 2a) and between  $\delta^{18}\text{O}$  values and  
 181 temperature (Fig. 2b) were weak ( $r^2 = 0.18$  and  $0.22$ , respectively), typical for islands  
 182 with a strong maritime influence (Bowen, 2008) where precipitation is likely a result of  
 183 a first condensate of water vapour from marine evaporation. Although the fit is poor,  
 184 the observed relationship between air temperature and  $\delta^{18}\text{O}$  values of precipitation  
 185 was approximately  $0.12$  per mil/  $^{\circ}\text{C}$ , significantly less than theoretical value of  $0.66$   
 186 per mil/  $^{\circ}\text{C}$  and observed values from continental locations (Dansgaard, 1964; Fricke &  
 187 O’Neil, 1999). The hydrogen and oxygen stable isotopic compositions of precipitation  
 188 were weakly seasonal, as were the amounts of precipitation (Fig. 2c), with amount  
 189 weighted monthly summer precipitation having slightly more positive  $\delta^2\text{H}$  and  $\delta^{18}\text{O}$   
 190 values than those of winter (Fig. 2d). This is most likely a consequence of the slight  
 191 temperature effect and the large annual temperature range ( $0\text{-}25$   $^{\circ}\text{C}$ ).

192 From these observations, the calculated mean annual amount weighted average  
 193  $\delta^2\text{H}$  and  $\delta^{18}\text{O}$  values of precipitation (MAP) on Sable Island are  $-37 \pm 12$  and  $-6.2 \pm$   
 194  $1.5$  per mil, respectively (Fig. 2d). These values were computed using all measurements  
 195 from the four years of our study, but we were missing samples from July to November  
 196 2020, thereby possibly biasing the MAP to winter precipitation and more negative  $\delta^2\text{H}$   
 197 and  $\delta^{18}\text{O}$  values. As a comparison, we also calculated annual amount weighted means  
 198 using interpolated values for the five months of missing data from the average values  
 199 for the existing three years of data yielding  $\delta^2\text{H}$  and  $\delta^{18}\text{O}$  values of  $-37 \pm 12$  and  $-6.1$   
 200  $\pm 1.6$  per mil. These values are indistinguishable within error from those calculated  
 201 using the incomplete data. This is not surprising considering the weak seasonality  
 202 differences between the summer and winter  $\delta^2\text{H}$  and  $\delta^{18}\text{O}$  values.

203 Both ordinary least squares and major axis regression of the  $\delta^2\text{H}$  and  $\delta^{18}\text{O}$  values  
 204 of integrated monthly precipitation resulted in a good fit to the data with major axis  
 205 regression having a higher deuterium intercept and slightly steeper slope than OSLR  
 206 models (Table 1). Weighting data points by precipitation amount resulted in a slightly  
 207 poorer fit, suggesting that the amount of precipitation does not significantly affect the  
 208 stable isotopic compositions of rainwater, as would be expected in a marine climate and  
 209 as observed on Figure 2a. This is also observed in the temporal profiles of D-excess  
 210 where there is no statistically significant periodicity (not shown);  $D_{ex}$  values across  
 211 all seasons remain relatively constant and average  $+12.2 \pm 2.7$  per mil. Ultimately  
 212 though, all regression models resulted in an almost identical fit within error (Fig. 3),  
 213 reflecting the open ocean climate of Sable Island, where high rainfall and cool moist  
 214 conditions result in minimal secondary evaporation of precipitation (Rozanski et al.,  
 215 1993).

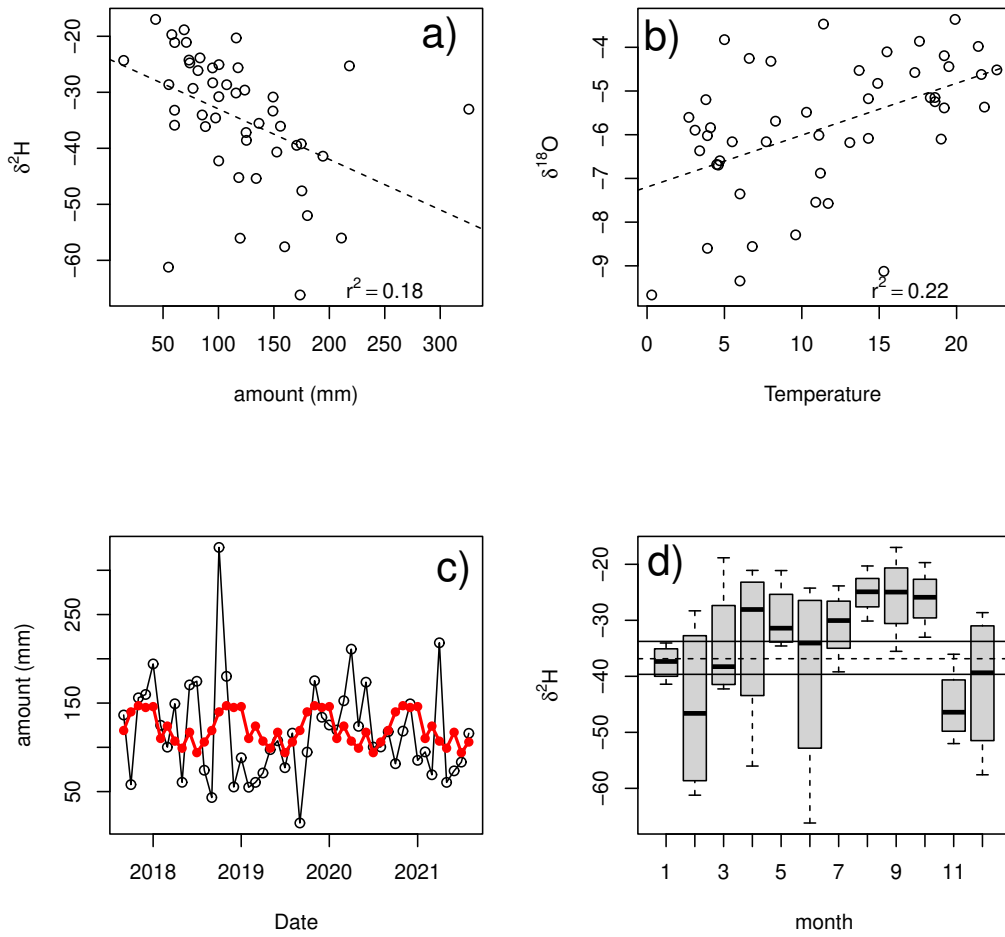


**Figure 2.** a.) Variation in  $\delta^2\text{H}$  values with precipitation amount and monthly temperature on Sable Island, NS, Canada from September, 2017 to August, 2021. b.) Variation in  $\delta^{18}\text{O}$  values of monthly precipitation with monthly mean temperature c.) Amounts of precipitation during the duration of this study. Shown in red are average precipitation amounts (Environment and Climate Change Canada, 2021). d.) Mean monthly  $\delta^2\text{H}$  values with amount weighted summer and winter precipitation values (upper and lower solid lines, respectively) and the mean annual amount weighted value (dashed line).



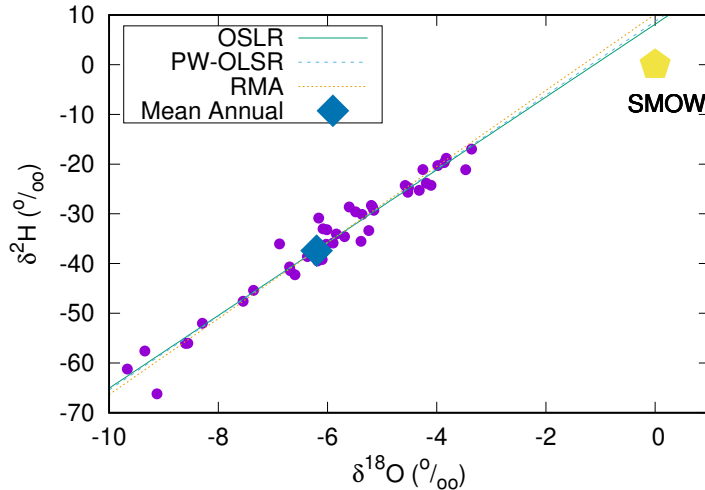


**Figure 3.** The relationship between  $\delta^2\text{H}$  and  $\delta^{18}\text{O}$  values of precipitation on Sable Island, NS, Canada from September, 2017 to August, 2021. Delta values are reported as per mil (‰) for both  $\delta^2\text{H}$  and  $\delta^{18}\text{O}$ . OLSR - Ordinary standard Linear regression, PW-OLSR - Precipitation Weighted – Ordinary Standard Linear Regression, RMA - Reduced Mean Axis regression, Mean Annual – amount weighted mean annual precipitation.

216

### 3.2 Seawater, surface, and groundwaters

217

218

219

220

221

222

Local seawater at Sable Island has relatively low  $\delta^2\text{H}$  and  $\delta^{18}\text{O}$  values of -13 and -2.6 per mil, respectively, considerably different from those of global average seawater values. This is consistent with the observations of LeGrande and Schmidt (2006) and reflects significant river input into the Arctic Ocean, North Sea, and Hudson Bay, the output of which contributes to the southward flowing Labrador current along the east coast of Canada, including Sable Island.

223

224

225

226

227

228

229

230

231

232

233

234

Shallow groundwater on Sable Island had a range of  $\delta^2\text{H}$  and  $\delta^{18}\text{O}$  values, from -44 to -12 (mean =  $-31 \pm 7$ ) per mil for hydrogen and -7.4 to -1.4 (mean =  $-5.7 \pm 1.3$ ) per mil for oxygen. The hydrogen and oxygen stable isotopic compositions of water from shallow groundwater wells all fall along the LMWL and are similar to the range of  $\delta^2\text{H}$  and  $\delta^{18}\text{O}$  values observed in local precipitation. It is also possible from a stable isotope perspective that these values are the result of mixing between local seawater to deep tap water at the main station (Fig. 4). Salinity of well waters were generally low, however, with most shallow wells having salinities of less than 1 ppt. This suggests that the variation in the  $\delta^2\text{H}$  and  $\delta^{18}\text{O}$  values likely reflects those of local precipitation rather than direct mixing. It is worth noting that a couple of the wells have salinities of up to 8-10 ppt Cl, indicating that incursion of seawater does occur into shallow groundwater in some instances.

235

236

237

238

239

240

These measurements support the model of Hennigar (1976) that groundwater on Sable Island consists of an elongated discontinuous freshwater lens that is recharged by infiltration of rainfall and diffuses out to the sea at the edges of the island. That direct mixing between groundwater and seawater may occur either by direct incursion or flooding of seawater during severe weather (Parker, 2018) is also consistent with our data.

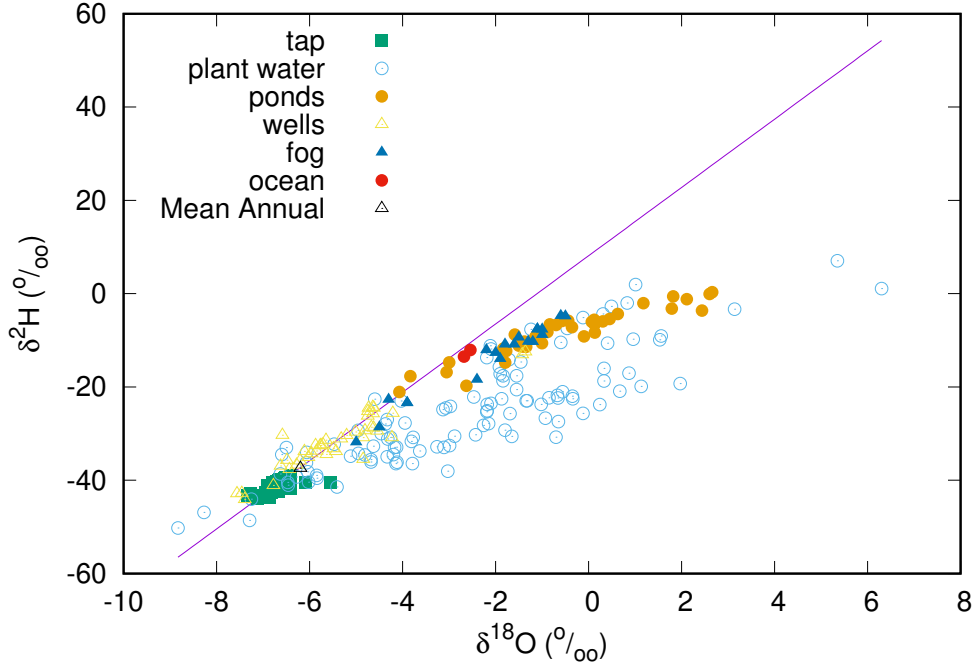


**Figure 4.** Hydrogen and oxygen stable isotopic compositions of deep groundwater, plant water, surface water, shallow groundwater, and fog from Sable Island, NS, Canada. Also shown are the Local Meteoric Water line (see Table 1) and the stable isotopic compositions of local seawater.

241 In contrast to shallow groundwater, groundwater from the deep well at the main  
 242 station has a relatively constant hydrogen and oxygen stable isotopic composition with  
 243  $\delta^2\text{H}$  and  $\delta^{18}\text{O}$  values of  $-41 \pm 1.3$  and  $-6.7 \pm 0.3$  per mil respectively. These values  
 244 are more negative than those of the mean annual precipitation or shallow groundwater  
 245 on the island and most probably indicate that recharge of the freshwater lens occurs  
 246 predominately in the winter. Indeed, calculated amount weighted mean winter pre-  
 247 cipitation  $\delta^2\text{H}$  values average -40 per mil (Fig. 2d), identical within analytical error to  
 248 those of deep groundwater.

249 The seasonality of groundwater recharge can be quantified based on the differ-  
 250 ences between groundwater stable isotopic compositions and those of amount-weighted  
 251 summer, winter, and annual precipitation (Jasechko et al., 2014). In this derivation,  
 252 the seasonal groundwater recharge bias can be expressed as:

$$\frac{(R/P)_{summer}}{(R/P)_{winter}} = \frac{\delta_{GW} - \delta_{summer}/\delta_{annual} - \delta_{summer}}{\delta_{GW} - \delta_{winter}/\delta_{annual} - \delta_{winter}} \quad (3)$$

253 where R/P is the recharge to precipitation ratio and GW, summer, winter, and annual  
 254 are the average delta values of groundwater, and the amount weighted average  
 255 delta values of summer, winter, and annual precipitation, respectively. The resultant  
 256 seasonal bias term,  $\frac{(R/P)_{summer}}{(R/P)_{winter}}$ , has values of less than one if summer recharge exceeds  
 257 winter recharge and of greater than one if *vice versa*.

258 For Sable Island, where the delta values of mean winter precipitation are es-  
 259 sentially identical to the groundwater values, the denominator of this calculation ap-

260 proaches zero, indicating that almost all of the groundwater is recharged by winter  
 261 precipitation with little or no contribution from summer precipitation. The ground-  
 262 water system on Sable Island has large discharge rates by which approximately 75%  
 263 of the available reservoir is lost into the sea annually by diffusion (Hennigar, 1976).  
 264 This, coupled with high evapotranspiration rates and lower precipitation amounts in  
 265 the summer, may reduce recharge in the summer to zero or even to negative rates, if  
 266 discharge exceeds input. Ponds and pools often disappear in the summer, indicating  
 267 a lowering of the water table and thus higher groundwater discharge than recharge.  
 268 We would also expect a seasonal variation in the stable isotopic compositions of main  
 269 station groundwater if summer recharge was significant, but that was not observed.

270 The intersection of the freshwater lens water table with the topography of Sable  
 271 Island results in standing pools, essentially surface exposures of the groundwater sys-  
 272 tem (Hennigar, 1976). These pools are typically ephemeral and can dry out completely  
 273 if the water table drops below the pond elevation. There is also observational evidence  
 274 of standing or perched ponds that have elevations above the water table, likely from  
 275 development of low permeability substrates (Hennigar & Kennedy, 2016).

276 The  $\delta^2\text{H}$  and  $\delta^{18}\text{O}$  values of these small ponds and pools can be compared to the  
 277 LMWL and mean annual precipitation values (Fig. 4). The  $\delta^2\text{H}$  and  $\delta^{18}\text{O}$  values of  
 278 the ponds range from -21 to 0 per mil and -4.1 to +2.6 per mil, respectively. The  $\delta^2\text{H}$   
 279 and  $\delta^{18}\text{O}$  values plot in as a linear cluster to the right of the LMWL, as a result of  
 280 isotopic enrichment typical of surface waters. A linear fit to this trend results in the  
 281 relationship  $\delta^2\text{H} = 2.92 \times \delta^{18}\text{O} - 6.80$  with a goodness of fit ( $r^2$ ) of 0.88.

282 This linear model intercepts the LMWL at  $\delta^2\text{H}$  and  $\delta^{18}\text{O}$  values of -17 and -3.4  
 283 per mil, values that are slightly more positive than those of the shallow wells and  
 284 significantly more positive than those of deep groundwater. This is an unexpected  
 285 result because considering that many of these pools are surface exposures of the local  
 286 groundwater, we would expect this intersection to reflect  $\delta^2\text{H}$  and  $\delta^{18}\text{O}$  values typical  
 287 of groundwater on the island. That they do not suggests that many of these small  
 288 pools and ponds are indeed isolated from the groundwater system, adding to existing  
 289 evidence that many of the pools on the island are standing or perched. These surface  
 290 waters were sampled in the summer when the water table is presumably at its lowest  
 291 adding to the probability of sampling these perched pools.

### 292 3.3 Plant Waters

293 Like surface waters, the hydrogen and oxygen stable isotopic compositions of  
 294 waters extracted from marram grass form a broad linear array to the right of the  
 295 LMWL (Fig. 4). The trend formed from the  $\delta^2\text{H}$  and  $\delta^{18}\text{O}$  values of plant water ( $\delta^2\text{H}$   
 296  $= 3.65 \times \delta^{18}\text{O} - 15.6$ ,  $r^2 = 0.744$ ) intersects the LMWL at more negative values than  
 297 does the similar, but parallel, trend formed from ponds and pools. The intersection  
 298 of this trend with the LMWL occurs at a  $\delta^2\text{H}$  and  $\delta^{18}\text{O}$  value of -37 and -6.2 permil  
 299 respectively, identical to  $\delta^2\text{H}$  and  $\delta^{18}\text{O}$  values of MAP and similar to those of shallow  
 300 groundwater on the island.

301 These results follow the same pattern as those observed in controlled experiments  
 302 by Millar et al. (2018) for plant water extracted from spring wheat (*Triticum aestivum*  
 303 *L.*). In these experiments, the  $\delta^2\text{H}$  and  $\delta^{18}\text{O}$  values of extracted plant water plot along  
 304 a trend with a shallow slope that intercepts the LMWL at values similar to the local  
 305 irrigation water.

### 306 3.4 Fog

307 Fog is prevalent in the summer on Sable Island but we were only able to collect  
 308 20 samples during the summers of 2018–2021 because high winds continually damaged

309 the fog collector. For the samples that were collected, fog had relatively positive  $\delta^2\text{H}$   
 310 and  $\delta^{18}\text{O}$  values that ranged from -32 to -4 per mil and -5.0 to -0.5 per mil, respectively  
 311 (Fig. 4), and plot close to those of local seawater. With the exception of a few relatively  
 312 negative values, these  $\delta^{18}\text{O}$  values are consistent with those observed previously by  
 313 Gonfiantini and Longinelli (1962) from the North Atlantic and most likely represent  
 314 a first stage condensate from water vapour in equilibrium with local seawater. In  
 315 agreement with a study of coastal fog described by Ingraham and Matthews (1990), the  
 316  $\delta^2\text{H}$  and  $\delta^{18}\text{O}$  values of fog plot slightly below the LMWL and have higher delta values  
 317 and lower  $D_{ex}$  values (mean = 3 per mil) than local rainfall. These low  $D_{ex}$  values most  
 318 likely are a result of equilibrium condensation of water vapour formed from evaporation  
 319 at very high relative humidity, consistent with the formation of fog.

320 The exceptions are a few fog samples that show more negative  $\delta^2\text{H}$  and  $\delta^{18}\text{O}$   
 321 values and plot on the LMWL (Fig. 4, 5). These likely represent mixed samples where  
 322 some rain was inadvertently collected by the fog collector on windy days. These sam-  
 323 ples also had the most positive  $D_{ex}$  values, further suggesting a component of rainwater.

324 Recently, it has been reported that non-rainfall events, such as dew, may display  
 325 a slightly different  $\delta^{17}\text{O} - \delta^{18}\text{O}$  relationship from other meteoric waters as a result  
 326 of non-equilibrium kinetic processes during formation although the sample size was  
 327 small (Kaseke et al., 2017). While radiation-induced and possibly advective fog from  
 328 the Nabib desert did not show any mass-independent fractionations between  $^{17}\text{O}$  and  
 329  $^{18}\text{O}$ , dew from the same location had measured  $^{17}\text{O}$ -excess values of about -120 per  
 330 meg (Kaseke et al., 2017), indicating that significant non equilibrium kinetic processes  
 331 occur during dew formation. Both advective dew and fog form from similar processes  
 332 involving the condensation of water vapour during contact with cold surfaces or air  
 333 masses. For this reason, we measured  $\delta^{17}\text{O}$  values of both fog and precipitation in  
 334 order to determine if there were any differences of the magnitude seen in previous  
 335 studies. We reasoned that if observed, these differences may ultimately allow us to  
 336 estimate the contribution of fog to other water reservoirs on the island. Unfortunately,  
 337 with laser based instruments, it is difficult to attain the precisions necessary for ac-  
 338 curate  $^{17}\text{O}$ -excess measurements ( $\pm 10$  per meg) without relatively long integration  
 339 times, advanced statistical analysis and sufficient numbers of repeated measurements  
 340 (Berman et al., 2013; Steig et al., 2014). However, even with the poor precisions of-  
 341 fered by these instruments ( $\sigma \approx \pm 100$  per meg) a large difference in mean values of  
 342  $^{17}\text{O}$ -excess, such as those previously seen between precipitation and dew, should be  
 343 detectable by the methods used.

344 For Sable Island, both rainfall and fog had  $^{17}\text{O}$ -excess values that ranged from  
 345 -176 to +197 per meg and had mean values that were not statistically different (Welch  
 346 T-test,  $p = 0.730$ ). This suggests that the formation of advective fog does not involve  
 347 significant non-equilibrium or kinetic processes and therefore  $^{17}\text{O}$ -excess values may  
 348 not be useful to determine the contribution of fog to the water budget or plant water  
 349 of Sable Island. However, it is possible that the relatively positive  $\delta^2\text{H}$  and  $\delta^{18}\text{O}$   
 350 values and low  $D_{ex}$  values of fog may allow some isotopic tracing. For example, fog  
 351 has similar stable isotopic compositions to those of ponds on the island but not to  
 352 those of groundwater or plant water (Fig 4), indicating it is possible that fog drip may  
 353 contribute to surface waters but not to groundwater.

## 354 4 Conclusions

355 This study presents the first dataset of the hydrogen and oxygen stable isotopic  
 356 compositions of precipitation (rain and fog), seawater, groundwater, plant water, and  
 357 surface water from Sable Island, NS, Canada. The  $\delta^2\text{H}$  and  $\delta^{18}\text{O}$  values of precipitation  
 358 in this marine dominated environment define a local meteoric water line described by  
 359  $\delta^2\text{H} = 7.32 \times \delta^{18}\text{O} + 8.13$ , with annual amount-weighted mean  $\delta^2\text{H}$  and  $\delta^{18}\text{O}$  values of

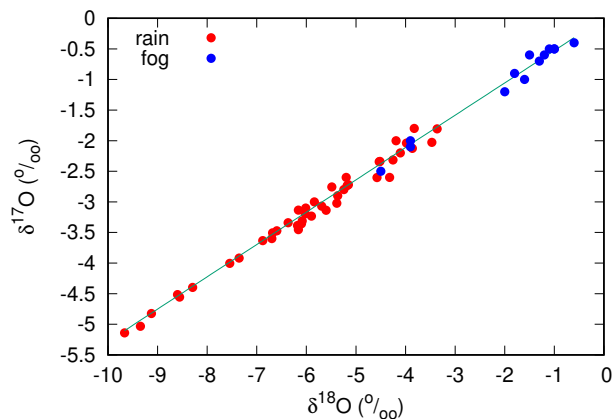


**Figure 5.** Relationship between  $\delta^{18}\text{O}$  and  $\delta^{17}\text{O}$  values in per mil (‰) for fog and rain samples on Sable Island, NS, Canada.

360 precipitation of  $-37 \pm 12$  and  $-6.2 \pm 1.7$  per mil, respectively. Seasonality in the stable  
 361 isotopic composition of precipitation is small but evident, where summer amount-  
 362 weighted precipitation have  $\delta^2\text{H}$  and  $\delta^{18}\text{O}$  values that are more positive than those in  
 363 the winter.

364 Stable isotopic compositions of groundwater from shallow wells reflect those of  
 365 precipitation but also may indicate that mixing between local seawater and ground-  
 366 water occurs locally either as a diffusional edge or as direct mixing from seawater  
 367 incursions during severe weather. Deep groundwater has hydrogen and oxygen stable  
 368 isotopic compositions that are similar to those of winter precipitation suggesting that  
 369 recharge of freshwater on the island occurs predominantly during the winter months  
 370 with little contribution from summer precipitation.

371 The  $\delta^2\text{H}$  and  $\delta^{18}\text{O}$  values of pools and ponds were more positive and offset from  
 372 those of precipitation indicating the usual evaporative enrichment of typical of surface  
 373 waters. From stable isotopic considerations, it is evident that while plants are fed  
 374 by local groundwater, many surface waters are likely isolated from the groundwater  
 375 system. In addition, it is possible that water from fog may contribute to surface waters.  
 376 In all, this is evidence of a precipitation-driven system with several distinct isotopic  
 377 pools.

378 Importantly, the existence of these distinct isotopic pools, such as fog and ground-  
 379 water, can allow the tracing of water to horses or other fauna on the island. These  
 380 data will also be of benefit to determine the water/plant sources to horses and may  
 381 also be used as a monitoring tool for water quality and quantity on the island. For  
 382 example, lower winter precipitation amounts as a result of climate change (Smith et  
 383 al., 2020) may reduce the amount of groundwater available to horses by lowering of  
 384 the water table.

## 385 5 Acknowledgments

386 This study was funded by Environment and Climate Change Canada. We thank  
 387 Sarah Medill and the Parks Canada staff for ongoing precipitation collections and  
 388 logistical support. Ruth Greuel and Phil McLoughlan graciously arranged transport  
 389 of samples from Sable Island to our laboratory and special thanks to Kim Janzen of

390 the Global Institute for Water Security at the UofS for her expertise with the plant  
391 water extractions.

## 392 6 Data Availability

393 All data used in this study will be publicly available the Government of Canada  
394 Open Data repository(ECCC, 2022) and through the GNIP program of the Interna-  
395 tional Atomic Energy Agency (IAEA) (IAEA/WMO, 2018).

## 396 References

- 397 Baxter, C. V., Fausch, K. D., & Carl Saunders, W. (2005). Tangled webs: reciprocal  
398 flows of invertebrate prey link streams and riparian zones. *Freshwater biol-*  
399 *ogy*, *50*(2), 201–220.
- 400 Berman, E. S., Levin, N. E., Landais, A., Li, S., & Owano, T. (2013). Measurement  
401 of  $\delta^{18}\text{O}$ ,  $\delta^{17}\text{O}$ , and  $^{17}\text{O}$ -excess in water by off-axis integrated cavity output  
402 spectroscopy and isotope ratio mass spectrometry. *Analytical chemistry*,  
403 *85*(21), 10392–10398.
- 404 Bowen, G. J. (2008). Spatial analysis of the intra-annual variation of precipita-  
405 tion isotope ratios and its climatological corollaries. *Journal of Geophysical Re-*  
406 *search: Atmospheres*, *113*(D5).
- 407 Clark, I. D., & Fritz, P. (1997). *Environmental isotopes in hydrogeology*. CRC press.
- 408 Craig, H. (1961). Isotopic variations in meteoric waters. *Science*, *133*(3465), 1702–  
409 1703.
- 410 Craig, H., & Gordon, L. I. (1965). Deuterium and oxygen 18 variations in the ocean  
411 and the marine atmosphere. In E. Tongiorgi (Ed.), (Vol. Stable Isotopes in  
412 oceanographic studies and paleotemperatures, p. 9-130). Consiglio nazionale  
413 delle ricerche, Laboratorio de geologia nucleare.
- 414 Crawford, J., Hughes, C. E., & Lykoudis, S. (2014). Alternative least squares meth-  
415 ods for determining the meteoric water line, demonstrated using GNIP data.  
416 *Journal of Hydrology*, *519*, 2331–2340.
- 417 Dansgaard, W. (1964). Stable isotopes in precipitation. *Tellus*, *16*(4), 436–468.
- 418 Eamer, J. B., Didier, D., Kehler, D., Manning, I., Colville, D., Manson, G. K., ...  
419 Kostylev, V. (2021). Multi-decadal coastal evolution of a North Atlantic shelf-  
420 edge vegetated sand island–Sable Island, Canada. *Canadian Journal of Earth*  
421 *Sciences*(ja).
- 422 ECCC. (2022). *Open Data*. <https://open.canada.ca/en/open-data>. Retrieved  
423 from <https://open.canada.ca/en/open-data>
- 424 Edwin, M., Lubis, S., Harahap, I. Y., Hidayat, T. C., Pangaribuan, Y., Sutarta,  
425 E. S., ... others (2014). Stable oxygen and deuterium isotope techniques to  
426 identify plant water sources. *Journal of Water Resource and Protection*, *6*(15),  
427 1501.
- 428 Environment and Climate Change Canada. (2021). *Historical Data - Climate -*  
429 *Environment and Climate Change Canada*. [http://climate.weather.gc.ca/](http://climate.weather.gc.ca/historical_data/search_historic_data_e.html)  
430 [historical\\_data/search\\_historic\\_data\\_e.html](http://climate.weather.gc.ca/historical_data/search_historic_data_e.html). (Accessed: 2021-12-05)
- 431 Epstein, S., & Mayeda, T. (1953). Variation of O-18 content of waters from natural  
432 sources. *Geochimica et Cosmochimica Acta*, *4*, 213–224.
- 433 Fischer, D. T., & Still, C. J. (2007). Evaluating patterns of fog water deposition  
434 and isotopic composition on the california channel islands. *Water Resources*  
435 *Research*, *43*(4).
- 436 Freedman, B., Catling, P. M., & Lucas, Z. (2011). Effects of feral horses on vegeta-  
437 tion of Sable Island, Nova Scotia. *The Canadian Field-Naturalist*, *125*(3), 200–  
438 212.
- 439 Fricke, H. C., & O’Neil, J. R. (1999). The correlation between 18o/16o ratios of  
440 meteoric water and surface temperature: its use in investigating terrestrial cli-

- mate change over geologic time. *Earth and Planetary Science Letters*, *170*(3), 181–196.
- Gonfiantini, R. (1986). Environmental isotopes in lake studies. *Handbook of environmental isotope geochemistry*, *2*, 113–168.
- Gonfiantini, R., & Longinelli, A. (1962). Oxygen isotopic composition of fogs and rains from the north atlantic. *Experientia*, *18*(5), 222–223.
- Gonfiantini, R., Wassenaar, L. I., Araguas-Araguas, L., & Aggarwal, P. K. (2018). A unified Craig-Gordon isotope model of stable hydrogen and oxygen isotope fractionation during fresh or saltwater evaporation. *Geochim Cosmochim Acta*.
- Gröning, M., Lutz, H., Roller-Lutz, Z., Kralik, M., Gourcy, L., & Pölsenstein, L. (2012). A simple rain collector preventing water re-evaporation dedicated for  $\delta^{18}\text{O}$  and  $\delta^2\text{H}$  analysis of cumulative precipitation samples. *Journal of Hydrology*, *448*, 195–200.
- Hennigar, T. W. (1976). *Water resources and environmental geology of sable island, nova scotia*. Department of the Environment, Water Planning and Management Division.
- Hennigar, T. W., & Kennedy, G. W. (2016). The precarious freshwater resources of Sable Island, Nova Scotia, Canada: Occurrence and management considerations. *Proceedings of the Nova Scotian Institute of Science (NSIS)*, *48*(2), 331.
- Hughes, C. E., & Crawford, J. (2012). A new precipitation weighted method for determining the meteoric water line for hydrological applications demonstrated using Australian and global GNIP data. *Journal of Hydrology*, *464*, 344–351.
- IAEA. (1992). *Statistical treatment of data on environmental isotopes in precipitation*. (Technical Series Report No. 331). IAEA Vienna.
- IAEA/WMO. (2018). *Global Network of Isotopes in Precipitation. The GNIP database*. Retrieved 2018-05-10, from [http://www-naweb.iaea.org/napc/ih/IHS{\\\_}resources{\\\_}gnip.html{\#}citing](http://www-naweb.iaea.org/napc/ih/IHS{\_}resources{\_}gnip.html{\#}citing)
- Ingraham, N. L., & Matthews, R. A. (1990). A stable isotopic study of fog: the point reyes peninsula, california, usa. *Chemical Geology: Isotope Geoscience section*, *80*(4), 281–290.
- Jasechko, S., Birks, S. J., Gleeson, T., Wada, Y., Fawcett, P. J., Sharp, Z. D., . . . Welker, J. M. (2014). The pronounced seasonality of global groundwater recharge. *Water Resources Research*, *50*(11), 8845–8867.
- Kaseke, K. F., Wang, L., & Seely, M. K. (2017). Nonrainfall water origins and formation mechanisms. *Science Advances*, *3*(3), e1603131.
- Koeniger, P., Marshall, J. D., Link, T., & Mulch, A. (2011). An inexpensive, fast, and reliable method for vacuum extraction of soil and plant water for stable isotope analyses by mass spectrometry. *Rapid Communications in Mass Spectrometry*, *25*(20), 3041–3048.
- LeGrande, A. N., & Schmidt, G. A. (2006). Global gridded data set of the oxygen isotopic composition in seawater. *Geophysical research letters*, *33*(12).
- McLoughlin, P. D., Lysak, K., Debeffe, L., Perry, T., & Hobson, K. A. (2016). Density-dependent resource selection by a terrestrial herbivore in response to sea-to-land nutrient transfer by seals. *Ecology*, *97*(8), 1929–1937.
- Meier-Augenstein, W. (2011). *Stable isotope forensics: an introduction to the forensic application of stable isotope analysis* (Vol. 3). John Wiley & Sons.
- Millar, C., Janzen, K., Nehemy, M. F., Koehler, G., Hervé-Fernández, P., & McDonnell, J. J. (2021). Organic contamination detection for isotopic analysis of water by laser spectroscopy. *Rapid Communications in Mass Spectrometry*, *35*(15), e9118.
- Millar, C., Pratt, D., Schneider, D. J., & McDonnell, J. J. (2018). A comparison of extraction systems for plant water stable isotope analysis. *Rapid Communications in Mass Spectrometry*, *32*(13), 1031–1044.

- 496 Morrison, J., Brockwell, T., Merren, T., Fourel, F., & Phillips, A. (2001). On-line  
497 high-precision stable hydrogen isotopic analyses on nanoliter water samples.  
498 *Analytical Chemistry*, *73*(15), 3570–3575.
- 499 Parker, S. (2018). *Supplemental Climate Information for Sable Island National Park*  
500 *Reserve* (Tech. Rep.). Parks Canada.
- 501 Plante, Y., Vega-Pla, J. L., Lucas, Z., Colling, D., De March, B., & Buchanan,  
502 F. (2007). Genetic diversity in a feral horse population from Sable Island,  
503 Canada. *Journal of Heredity*, *98*(6), 594–602.
- 504 R Core Team. (2015). R: A language and environment for statistical computing  
505 [Computer software manual]. Vienna, Austria. Retrieved from [https://www.R-](https://www.R-project.org/)  
506 [project.org/](https://www.R-project.org/)
- 507 Richardson, D. H., Lucas, Z., & Anderson, F. (2009). The lichen flora of Sable Is-  
508 land, Nova Scotia: Its past, present and likely future status. *The Bryologist*,  
509 *112*(3), 558–571.
- 510 Rozanski, K., Araguás-Araguás, L., & Gonfiantini, R. (1993). Isotopic patterns in  
511 modern global precipitation. *Climate change in continental isotopic records*, 1–  
512 36.
- 513 Schoenemann, S. W., Schauer, A. J., & Steig, E. J. (2013). Measurement of SLAP2  
514 and GISP  $\delta^{17}\text{O}$  and proposed VSMOW-SLAP normalization for  $\delta^{17}\text{O}$  and  
515  $^{17}\text{O}$ -excess. *Rapid Communications in Mass Spectrometry*, *27*(5), 582–590.
- 516 Smith, D. M., Scaife, A. A., Eade, R., Athanasiadis, P., Bellucci, A., Bethke, I., ...  
517 others (2020). North atlantic climate far more predictable than models imply.  
518 *Nature*, *583*(7818), 796–800.
- 519 Stalter, R., & Lamont, E. E. (2006). The historical and extant flora of Sable Island,  
520 Nova Scotia, Canada. *The Journal of the Torrey Botanical Society*, *133*(2),  
521 362–374.
- 522 Steig, E., Gkinis, V., Schauer, A., Schoenemann, S., Samek, K., Hoffnagle, J., ...  
523 Tan, S. (2014). Calibrated high-precision  $^{17}\text{O}$ -excess measurements using  
524 cavity ring-down spectroscopy with laser-current-tuned cavity resonance. *At-*  
525 *mospheric Measurement Techniques*, *7*(8), 2421–2435.
- 526 Tian, C., Jiao, W., Beysens, D., Kaseke, K. F., Medici, M.-G., Li, F., & Wang, L.  
527 (2021). Investigating the role of evaporation in dew formation under different  
528 climates using  $^{17}\text{O}$ -excess. *Journal of Hydrology*, *592*, 125847.
- 529 Tissier, E. J., McLoughlin, P. D., Sheard, J. W., & Johnstone, J. F. (2013). Distribu-  
530 tion of vegetation along environmental gradients on Sable Island, Nova Scotia.  
531 *Écoscience*, *20*(4), 361–372.
- 532 Vander Zanden, H. B., Soto, D. X., Bowen, G. J., & Hobson, K. A. (2016). Expand-  
533 ing the isotopic toolbox: applications of hydrogen and oxygen stable isotope  
534 ratios to food web studies. *Frontiers in Ecology and Evolution*, *4*, 20.
- 535 Wolf, B. O., Martínez del Rio, C., & Babson, J. (2002). Stable isotopes reveal that  
536 saguaro fruit provides different resources to two desert dove species. *Ecology*,  
537 *83*(5), 1286–1293.
- 538 Yurtsever, Y., & Gat, J. (1981). *Atmospheric waters. Stable isotopes hydrology,*  
539 *deuterium and oxygen-18 in the water cycle.* IAEA (Tech. Rep.). Vienna, Tech  
540 Rep Ser.